

symmetry, $c \approx 3 \times 4.6\text{Å}$). A new nigerite polytype, with trigonal symmetry and $c = 56.2\text{Å}$, was identified by Peacor (1967). In McKie's nomenclature this is a 12R polytype, but Peacor suggested that a more realistic nomenclature system should be based on a single oxygen layer repeat to account for odd-layer number repeats, e.g. davidite (Rouse and Peacor, 1968). Using this system the two nigerite polytypes are 6H and 24R respectively. In the present paper we adhere to Peacor's suggested nomenclature system.

In a recent mineralogical examination of polished sections from a tin-bearing magnetite-fluorite-biotite deposit from Mt. Garnet in northern Queensland, we confirmed the presence of a tin-rich aluminum oxide, which had been observed in earlier studies on the deposit (H.W. Fander, private communication, 1976). Single crystals of the phase were excavated from the polished sections and studied by precession and Weissenberg X-ray diffraction methods. These studies, coupled with microprobe analyses, served to characterize the mineral as a 24R nigerite polytype, analogous to the mineral described by Peacor (1967). We report here the single-crystal structure determination for nigerite-24R, and use the results to predict the structures of some polytypes in the related series—nigerite, högbomite, taafeite.

Experimental

Drill-core sections containing nigerite were kindly supplied by Mr. L. A. Newnham, chief geologist at Renison Limited in Tasmania. The samples were from a drilling program carried out by Comalco Ltd. at their Mt. Garnet tin deposits in northern Queensland. In polished section the nigerite appeared as small rods and plates, generally 5–50 μm wide and up to $\sim 100 \mu\text{m}$ long, in a matrix comprising colloform-banded magnetite with fluorite and biotite. Associated minerals included gahnite, corundum, and cassiterite. The elongated lath-like nigerite crystals were often intergrown at an angle of about 120° . Examination of the crystals in a scanning electron microscope fitted with an energy-dispersive analyzer showed dominant Al, Sn, together with minor Fe, Zn, and trace amounts of Ca, Mn.

Crystals excavated from the polished section appeared colorless under the binocular microscope and a very pale green in transmitted light. An elongated tabular crystal measuring $77 \times 35 \times 20 \mu\text{m}$ was selected for the X-ray diffraction study. Initially, precession and Weissenberg photographs were used to confirm that it was a single crystal, with trigonal sym-

metry, $R3m$, $R32$, or $R\bar{3}m$, and approximate cell dimensions $a = 5.73$, $c = 55.6\text{Å}$.

For the intensity data collection the crystal was remounted along its long dimension on a Philips PW1100 4-circle automatic diffractometer. Thirteen reflections with $14^\circ < 2\theta < 29^\circ$ were carefully centered and the 2θ values used in a least-squares refinement to calculate the lattice parameters as reported in Table 1. Intensities were collected with graphite-monochromated $\text{MoK}\alpha$ radiation. A θ - 2θ scan, 3–30°, was used with a variable scan width given by $\Delta\theta = (0.9 + 0.3 \tan \theta)$ and a speed of $0.03^\circ \text{sec}^{-1}$. Two background measurements, each for half the scan time, were made for each scan, one at the lower and one at the upper limit. The intensities were processed using a program written for the PW 1100 diffractometer by Hornstra and Stubbe (1972). An absorption correction was not applied. However, a partial compensation was achieved by averaging the intensities of equivalent reflections, $\pm(hkl, lhk, klh)$, in the rhombohedral cell. (Interscale R factor for equivalent reflections = 0.054.) Thus, the 2834 reflections measured were reduced to a unique set of 656, of which 477 had $F^2 \geq 3\sigma [F^2]$ and were used in the structure refinement.

Scattering factor curves for Sn, Fe, Al, Ca, Zn, and Mn neutral atoms are those of Cromer and Mann (1968). Anomalous dispersion corrections for all atoms are from Cromer and Liberman (1970). All computing was performed on the Monash University CDC 3200 and Burroughs 6700 and the CSIRO CDC 7600 computers.

Two nigerite grains in close proximity to the one excavated for XRD studies were subjected to microprobe analyses. The results (given in Table 2) show variations of up to 10 percent in individual element analyses; the two data sets were averaged to obtain a typical analysis applicable to the XRD crystal. The derived unit-cell composition, normalized to 32 anions, is given in Table 2.

A structural model for nigerite and related mineral polytype—general considerations

The diffraction patterns for nigerite and related mineral polytypes are dominated by strong spinel-like subcell reflections. In the case of the nigerite-24R described here, the strongest reflections define a 6R type sublattice with $a = 5.73$, $c = 13.90\text{Å}$. For comparison the unit cell for the spinel gahnite, when referred to hexagonal axes, is also 6R in type and has $a = 5.73$, $c = 14.04\text{Å}$. As a consequence the three-dimensional Patterson map for nigerite showed only

Table 1. Nigerite-24R: unit-cell parameters

a_{rh}	= 18.826(10) Å	a_{hex}	= 5.730(3) Å
α_{rh}	= 17.508(3)°	c_{hex}	= 55.60(3) Å
Z_{rh}	= 1	Z_{hex}	= 3
Space group $R\bar{3}m$			
D_{calc}	= 4.42 g cm ⁻³		
μ	= 70.4 cm ⁻¹		

spinel-type subcell vectors, and was thus not very useful in helping to establish a structural model. However, the similarities in the diffraction data and unit-cell parameters for nigerite, högbomite, and taaffeite polytypes suggested that a simple structural principle, such as intergrowth of two basic structure types, should relate the structures of the various polytypes. An attempt was thus made to solve the structure of nigerite-24R by using crystallochemical reasoning to establish the underlying general structural principle for the polytypes. In this approach we were aided by the available structural information for nigerite and related minerals, as well as published data for related compounds with known structures.

Initially, a survey was made of compounds with known structures, containing close-packed oxygen frameworks, which could be described by hexagonal/trigonal unit cells with $a \approx 5.7$, $c \approx n \times 2.3A$. [Compounds with large cations occupying anion sites, such as various ferrites, e.g. BaFe₁₂O₁₉ (Townes *et al.*, 1967), were not considered because the nigerite-högbomite-taaffeite polytypes do not contain such ions.] In addition to spinel, with cubic stacking of close-packed oxygen layers, (c...), $n = 6$, there are a number of compounds with double-hexagonal stacking, *i.e.* (ch...), $n = 4$, and also series of compounds with simple hexagonal stacking of the oxygen layers, (h...), $n = 2$. The former are typified by the mineral nolanite, an iron vanadate, (Fe,V)₅O₈ (Hanson, 1958), and also by compounds A₂Mo₃O₈, A = Zn, Mg, Mn... (McCarroll *et al.*, 1957), and the simple hexagonal structures are represented by the series LiRMO₃O₈, R = Sc, Y, In, Sm... (McCarroll, 1977). The three types of structures, designated (c...), (ch...), and (h...) according to the oxygen layer stacking, (ABC...), (ABAC...) (AB...) respectively, have some important features in common. For instance, the layer of octahedrally coordinated metal atoms as shown in Figure 1(i) occurs in all three structures and

alternates with layers containing both octahedrally and tetrahedrally coordinated metal atoms [Figs. 1(ii) and 1(iii)]. To simplify the discussion we have designated these layers as O (for octahedral cations only), T₂ (two tetrahedral cations per layer in the unit cell), and T₁ (one tetrahedral cation) respectively [Fig. 1, (i)-(iii)]. For spinel, O and T₂ layers alternate, whereas in both the (ch...) and (h...) structures O and T₁ metal atom layers alternate along [0001]. The interlayer articulation of polyhedra (*i.e.* between metals in the O and T layers) depends on the oxygen stacking sequence. Octahedron-octahedron articulation occurs by edge-sharing only in (c...), by corner-sharing only in (h...), and by both corner- and edge-sharing in (ch...). These are shown in Figure 2. Tetrahedron-octahedron articulation occurs only by corner-sharing in both the (c...) and (ch...) structures, and by corner- and edge-sharing (as in olivine) in the (h...) structures (see Fig. 3). Note that this latter type of tetrahedron-octahedron articulation is avoided in the (ch...) structures by having only one of the two available tetrahedral sites in the T₁ layers occupied.

The unit-cell compositions of the O, T₂, and T₁ layers (including surrounding oxygens) are M₃O₄, M₃O₄, and M₂O₄ respectively, and so the overall compositions of the (c...), (ch...), and (h...) type compounds (normalized to 8 oxygens for comparison) are M₆O₈, M₆O₈, and M₅O₈ respectively. It follows that long-periodicity structures with mixed stacking sequences, e.g. cchccchh..., will have compositions intermediate to M₅O₈ and M₆O₈. This in fact is true for all the known polytypes of nigerite, högbomite, and taaffeite, range M_{5.297}O₈ to M₆O₈ (McKie, 1963; Hudson *et al.*, 1967; Wilson, 1977). We were able to es-

Table 2. Nigerite-24R: electron microprobe analyses

	Weight percent		Atoms*	
	1	2**	1	2
Al	27.78	27.93	14.66	14.73
Sn	17.62	15.89	2.11	1.91
Fe	10.50	11.12	2.68	2.83
Zn	6.23	6.81	1.36	1.48
Ca	0.81	0.75	0.29	0.27
Mn	0.26	0.25	0.07	0.06
Si	0.40	0.43	0.20	0.22

* Number of atoms per unit cell, normalized to 30 O + 2 OH, and with all iron as ferrous. The averaged unit cell composition from 1 and 2 is Al_{14.69}Sn_{2.01}Fe_{2.76}Zn_{1.42}Ca_{0.28}Mn_{0.06}Si_{0.21}O₃₀(OH)₂.

** 1 and 2 are point analyses for two different grains.

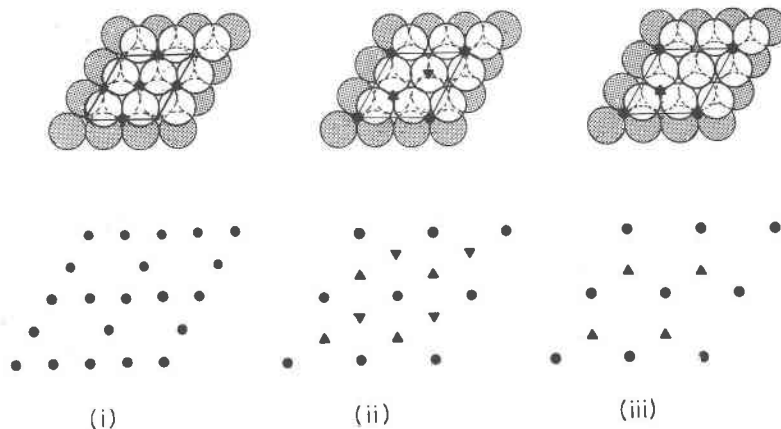


Fig. 1. Metal atom arrangements between close-packed oxygen layers for (i) the O layer in spinel and nolanite, (ii) the T_2 layer in spinel, and (iii) the T_1 layer in nolanite. The small solid circles and triangles represent octahedrally and tetrahedrally coordinated metals, respectively. Oxygen layers and unit-cell outlines are shown in the upper parts of the figure; the lower half shows the extended metal atom arrangements.

establish the correct structural model for nigerite-24R, and predict models for other polytypes, on the basis that they were built up from a stacking of O, T_2 , and T_1 layers, the sequence being determined by the oxygen-layer stacking scheme. This is outlined below.

Model for nigerite-24R

Using the realistic assumption that the c -axis periodicity ($n = 24$) is determined by the oxygen stacking sequence (rather than by subtle changes in metal atom ordering), the possible layer sequences may be

obtained from Patterson and Kasper's Table in *International Tables for X-ray Crystallography*, Vol. II (1962), p. 342–355. Nigerite-24R has an even period, $N = 8$, and a primitive rhombohedral lattice, and the appropriate table shows that eight different stacking sequences are possible. These were reduced to two probable sequences using the criterion that cubic stacking should predominate, as suggested by the strong spinel-like subcell. These two possibilities are designated (6)(2) and (5)(3) by Patterson and Kasper and comprise stacking sequences (ccccchch...) and (ccccchcch...). The observation of an even number of layers for nigerite-24R (as indeed is the case for all the reported polytypes of nigerite, högbomite, and taaffeite) required that O and T metal atom layers alternate. A further restriction suggested by the survey of known related structures given above was that T_2 layers lay between pairs of cubic stacked oxygen layers, i.e. $c-T_2-c$, and T_1 layers lay between cubic- and

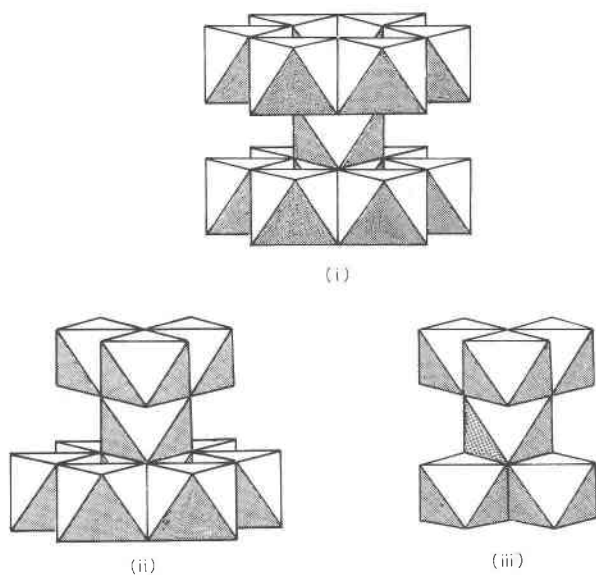


Fig. 2. Polyhedral representations of interlayer articulation of octahedra in (i) LiRMO_3O_8 , (ii) nolanite, and (iii) spinel-type structures.

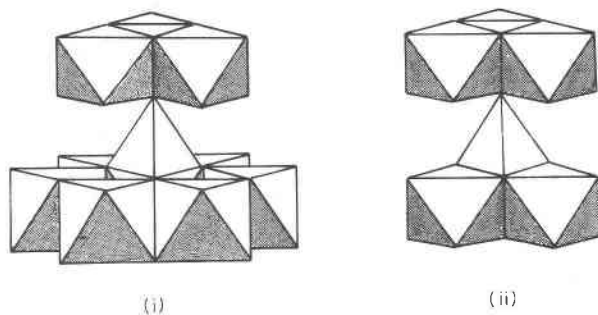


Fig. 3. Polyhedral representations of interlayer articulation of tetrahedra and octahedra in (i) LiRMO_3O_8 and (ii) spinel and nolanite type structures.

Table 3. Nigerite-24R: final atomic coordinates and isotropic temperature factors

Atom site	Occupancy	x	y	z	B (\AA^2)
M(1) OCT.	2.1 Al + 0.9 □*	0.50000	0.00000	0.50000	0.24(10)
M(2) OCT.	2 Sn	0.28684(2)	0.28684(2)	0.28684(2)	0.31(2)
M(3) TET.	1.2 Al + 0.8 Fe	0.03070(6)	0.03070(6)	0.03070(6)	0.52(6)
M(4) OCT.	6 Al	0.75013(7)	0.75013(7)	0.25328(14)	0.35(5)
M(5) OCT.	2 Al	0.12488(8)	0.12488(8)	0.12488(8)	0.22(9)
M(6) TET.	Fe + 0.8 Zn + 0.2 Al	0.53153(4)	0.53153(4)	0.53153(4)	0.39(4)
M(7) TET.	Fe + 0.6 Zn + 0.4 Al	0.22047(5)	0.22047(5)	0.22047(5)	0.66(5)
M(8) OCT.	3 Al	0.00000	0.00000	0.50000	0.33(8)
O(1)	6 O	0.1558(2)	0.1558(2)	0.6257(3)	0.94(15)
O(2)	2 OH	0.3504(2)	0.3504(2)	0.3504(2)	0.91(25)
O(3)	6 O	0.4420(2)	0.4420(2)	0.9213(3)	0.98(15)
O(4)	2 O	0.0644(2)	0.0644(2)	0.0644(2)	0.88(25)
O(5)	6 O	0.0439(2)	0.0439(2)	0.6026(3)	0.82(13)
O(6)	2 O	0.5666(2)	0.5666(2)	0.5666(2)	0.26(22)
O(7)	6 O	0.7056(2)	0.7056(2)	0.1467(3)	0.97(14)
O(8)	2 O	0.1844(2)	0.1844(2)	0.1844(2)	0.72(24)

* = vacancy

Table 4. Nigerite-24R: selected interatomic distances (Å) and angles (degrees)

M(1) (Al) Octahedron				M(5) (Al) Octahedron			
M(1)-O(1)	1.982*(x4)	O(1)-M(1)-O(2)	84.73 (x4)	M(5)-O(5)	1.894 (x3)	O(7)-M(5)-O(7)'	82.22 (x3)
M(1)-O(2)	1.908 (x2)	O(1)-M(1)-O(1)'	85.56 (x2)	M(5)-O(7)	1.922 (x3)	O(5)-M(5)-O(5)'	83.79 (x3)
Mean	1.957	O(1)-M(1)-O(1)''	94.44 (x2)	Mean	1.908	O(5)-M(5)-O(7)	96.99 (x6)
		O(1)''-M(1)-O(2)	95.27 (x4)				
O(1)-O(2)	2.622 (x4)			O(7)-O(7)'	2.527 (x3)		
O(1)-O(1)'	2.693 (x2)			O(5)-O(5)'	2.529 (x3)		
O(1)-O(1)''	2.910 (x2)			O(5)-O(7)	2.858 (x6)		
O(1)''-O(2)	2.875 (x4)						
M(2) (Sn) Octahedron				M(6) (Fe,Zn) Tetrahedron			
M(2)-O(1)	2.108 (x3)	O(1)-M(2)-O(1)'	79.38 (x3)	M(6)-O(6)	1.949	O(7)-M(6)-O(7)'	108.73 (x3)
M(2)-O(3)	2.003 (x3)	O(1)-M(2)-O(3)	91.59 (x6)	M(6)-O(7)	1.970 (x3)	O(6)-M(6)-O(7)	110.21 (x3)
Mean	2.056	O(3)-M(2)-O(3)'	96.26 (x3)	Mean	1.965		
O(1)-O(1)'	2.692 (x3)			O(7)-O(7)'	3.203 (x3)		
O(1)-O(3)	2.948 (x6)			O(6)-O(7)	3.215 (x3)		
O(3)-O(3)'	2.984 (x3)						
M(3) (Al,Fe) Tetrahedron				M(7) (Fe,Zn) Tetrahedron			
M(3)-O(1)	1.837 (x3)	O(1)-M(3)-O(1)'	111.57 (x3)	M(7)-O(5)	1.925 (x3)	O(5)-M(7)-O(8)	106.22 (x3)
M(3)-O(4)	1.873	O(1)-M(3)-O(4)	107.28 (x3)	M(7)-O(8)	2.005	O(5)-M(7)-O(5)'	112.52 (x3)
Mean	1.846			Mean	1.945		
O(1)-O(4)	2.987 (x3)			O(5)-O(8)	3.144 (x3)		
O(1)-O(1)'	3.037 (x3)			O(5)-O(5)'	3.201 (x3)		
M(4) (Al) Octahedron				M(8) (Al) Octahedron			
M(4)-O(3)	1.879 (x2)	O(5)-M(4)-O(5)'	80.37	M(8)-O(7)	1.898 (x4)	O(7)-M(8)-O(8)	82.58 (x4)
M(4)-O(6)	1.923	O(3)-M(4)-O(6)	82.97 (x2)	M(8)-O(8)	1.926 (x2)	O(7)-M(8)-O(7)	83.50 (x2)
M(4)-O(4)	1.936	O(4)-M(4)-O(5)	83.95 (x2)	Mean	1.907	O(7)-M(8)-O(7)''	96.50 (x2)
M(4)-O(5)	1.960 (x2)	O(3)-M(4)-O(5)	92.82 (x2)			O(7)''-M(8)-O(8)	97.42 (x4)
Mean	1.923	O(3)-M(4)-O(3)'	93.92	O(7)-O(8)	2.523 (x4)		
O(5)-O(5)'	2.529	O(5)-M(4)-O(6)	95.63 (x2)	O(7)-O(7)'	2.527 (x2)		
O(3)-O(6)	2.519 (x2)	O(3)-M(4)-O(4)	97.40 (x2)	O(7)-O(7)''	2.832 (x2)		
O(4)-O(5)	2.605 (x2)			O(7)''-O(8)	2.873 (x4)		
O(3)-O(5)	2.781 (x2)						
O(3)-O(3)'	2.747						
O(5)-O(6)	2.877 (x2)						
O(3)-O(4)	2.866 (x2)						

* Standard deviations for M-M, M-O, and O-O are 0.003, 0.005, and 0.008 Å, respectively, and for angle O-M-O 0.16 degrees.

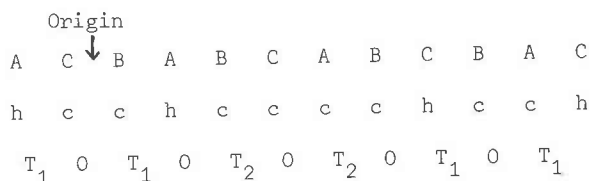


Fig. 4. Anion layer sequence (first two lines) and metal atom layer sequence (third line) for nigerite-24R.

hexagonal-stacked oxygen layers, *i.e.* c-T₁-h. It was also possible to make some reasonable assumptions concerning the metal atom distributions in the trial models. Firstly, by analogy with gahnite, it was expected that the spinel-like slabs would contain aluminum in octahedral sites and large divalent ions, Zn²⁺ and Fe²⁺, in the tetrahedral sites. Secondly, Sn⁴⁺ has a marked preference for octahedral coordination in spinel (Djega-Mariadassou *et al.*, 1973). It is not expected to order with the much smaller Al³⁺ in the O layers and was thus assigned to T₁ layers.

Subject to the restrictions outlined above, only a small number of models remained to be tested. Structure factor calculations for these possible models indicated a centrosymmetric model (*R*3̄*m*), with the (5)(3) oxygen stacking sequence as correct.

Refinement of the structure

The origin location was established in the space group *R*3̄*m* by assigning O-layer metals (aluminums) to the special positions 3(*e*) and 3(*d*), *i.e.* 0 ½ ½ and ½ 0 0 (rhombohedral axes). Initially, with Al atoms assigned to the O-layers and an average structure factor curve for M atoms in the T layers, full refinement of coordinates of all atoms proceeded smoothly to an *R* of about 0.15. At this stage, a difference Fourier and temperature factor refinement allowed a specific assignment of Sn, Fe, *etc.* to the different metal atom sites in the T layers. With a new set of scattering curves, refinement of all coordinates and isotropic temperature factors proceeded to an *R* value of 0.065. The refined temperature factors showed a wide range of values, from -0.40(20) to 1.57(33), and a difference Fourier displayed a number of peaks of density greater than 2e Å⁻², in unrealistic positions (*e.g.* within ~2Å from metal atoms). Examination of the structure factor table showed that 30 of the weakest reflections (3σ[F²] < F² < 4σ[F²]) had F_o values systematically higher than F_c by a factor of 2 or more. These reflections were given zero weight in the subsequent refinement. Further cycles of full matrix refinement of positional and isotropic thermal param-

eters led to convergence at *R* = 0.044, *wR* = 0.033, and *R*(F²) = 0.058, for 448 observed reflections. The refined atomic coordinates (in the rhombohedral cell) and thermal parameters are listed in Table 3. The thermal parameters for oxygens are now within the narrow range expected for a close-packed oxide [except for O(6), which had a B value of -0.40(20) before removal of the 30 affected reflections]. A final difference Fourier showed no features above 0.5eÅ⁻².

Calculated bond lengths are given in Table 4 and observed and calculated structure factors are listed in Table 5.¹

Description of the structure

The structure of nigerite is based on a close-packed oxygen framework with a 24-layer repeat along the hexagonal *c* axis (8-layer true repeat in the primitive rhombohedral cell). The layer sequence is shown in Figure 4, together with the stacking representation for each oxygen layer (c or h) and the metal atom layer sequence. The oxygen sequence is (cchccccch...) and the metal atom layer sequence is (OT₁OT₁OT₂OT₂...). The... OT₂OT₂... sequence represents a four-layer slab of spinel structure. The ...OT₁OT₁... metal layer sequence is the same as that for the double-hexagonal-close-packed nolanite structure, and the O-T₁-O interlayer polyhedral articulations are the same [see Figs. 2(ii) and 3(i)]. However, the oxygen layer sequence is different, *viz.* hcch for nigerite and hchc for nolanite, and this results in different T₁-O-T₁ interlayer polyhedral linkages, as shown in Figure 5, which gives a polyhedral representation corresponding to the asymmetric unit in the triply-primitive hexagonal cell. The O, T₁, and T₂ layers are marked, as well as the various metal atoms. For convenience in interpreting Figure 5, the atomic coordinates have been converted to those pertaining to the hexagonal cell and are given in Table 6. To show the magnitude of the various deviations from an ideal close-packed model, the *z* parameters are also given in angstroms. It is apparent that there are considerable distortions both in the planarity of the oxygen layers, and in the close packing of the oxygens within the layers. For example, the ideally coplanar O(1) and O(2) atoms differ by more than 0.2Å in their *z* parameter, and the *y* parameters of O(5) and O(7) also differ by more than 0.2Å from the

¹ To obtain a copy of Table 5, order Document AM-79-115 from the Business Office, Mineralogical Society of America, 2000 Florida Avenue, NW, Washington, D.C. 20009. Please remit \$1.00 in advance for the microfiche.

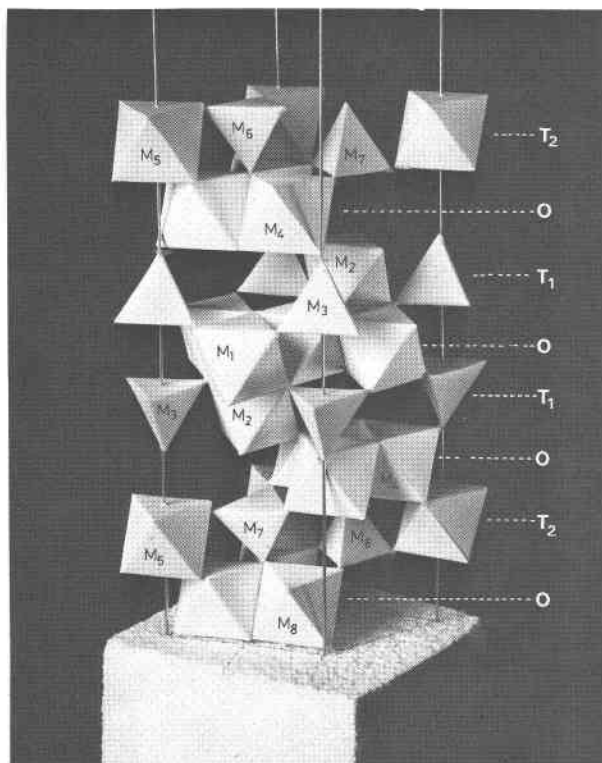


Fig. 5. Polyhedral model of nigerite-24R in a hexagonal cell representation.

ideal values ($y = 5/6$ and $2/3$ respectively). The octahedral metal M(2) (tin) in the T_1 layer shows a displacement of 0.27\AA , whereas the metals in the O layers are almost exactly midway between the sandwiching oxygen layers.

Metal atom ordering

Metal atom ordering in a number of sites is quite unambiguous. In particular the octahedral site in the T_1 layers is fully occupied by tetravalent tin. The average $\text{Sn}^{2+}\text{-O}$ bond length of $2.056(5)\text{\AA}$ agrees with a calculated value of 2.06\AA , using Shannon and Prewitt's (1969) ionic radii tables. (The oxygen radius appropriate to the average coordination number 3.5 was used.) The ordering of Al into the octahedral sites in the spinel block is also clearly established from the structure refinement. The observed $\overline{\text{Al-O}}$ bond lengths of $1.908(5)$ [M(5) in T_2 layer] and $1.907(5)$ [M(8) in O layer] and $1.923(5)$ [M(4) in O layer] lie within the range $1.885\text{--}1.924$ observed for Al atoms in the octahedral sites in the spinel blocks of various β -aluminas (e.g. Dernier and Remeika, 1976; Kodama and Muto, 1976). In fact the spinel block in nigerite resembles quite closely gahnite, ZnAl_2O_4 (Saalfeld, 1964), on which nigerite is often

found as an overgrowth. Complete correspondence requires divalent ions Fe^{2+} , Zn^{2+} in the tetrahedral sites, whereas the observed average bond lengths (Table 3) suggest some trivalent Al in these sites. Note the opposite senses of the ratios of the apical to basal M-O bond lengths for the two tetrahedral sites, M(6) and M(7), in the spinel block.

A difficulty was encountered in determining the occupancy of the octahedral site M(1) in the O layer. With Al assigned to this site, a reasonable temperature factor was obtained only when the occupancy was reduced to 0.70 (Table 3). The average M(1)-O bond length, $1.957(5)\text{\AA}$, is somewhat higher than expected for Al, reflecting a lower average polyhedral bond strength due to the partial occupancy. Allowance for iron in this site would decrease the partial occupancy parameter still further.

Whereas in the T_2 layers small ions (Al^{3+}) occupy the octahedral site and large ions (Fe^{2+} , Zn^{2+}) occupy the tetrahedral sites, the reverse is true in the T_1 layers, with large octahedral Sn^{4+} and small tetrahedral Al^{3+} . As a consequence of adjusting to the various-sized polyhedra, the $\text{M}(4)\text{O}_6$ octahedra in the intervening O layer are considerably distorted, with M(4)-O bond lengths in the range $1.879(5)\text{--}1.960(5)\text{\AA}$. By comparison, the $\text{M}(8)\text{O}_6$ octahedra in the O layers in the spinel block are more regular, with a M(8)-O range of $1.898(5)\text{--}1.926(5)\text{\AA}$.

Table 6. Nigerite-24R: atomic coordinates in the hexagonal cell representation

Atom site	Atom type	Fractional coordinates			z (\AA)	Layer type
		x	y	z		
M(1)	Al	$\frac{1}{2}$	0	0	0.00	0
O(1)	O	0.8233	0.6466	0.0210	1.17	c
O(2)	OH	$\frac{1}{3}$	$\frac{2}{3}$	0.0171	0.95	
M(2)	Sn	$\frac{2}{3}$	$\frac{1}{3}$	0.0465	2.59	
M(3)	Al, Fe	0	0	0.0307	1.71	T_1
O(3)	O	0.4931	0.9862	0.0649	3.61	h
O(4)	O	0	0	0.0644	3.58	
M(4)	Al	0.1677	0.3355	0.0822	4.57	0
O(5)	O	0.8529	0.7058	0.1032	5.74	c
O(6)	O	$\frac{1}{3}$	$\frac{2}{3}$	0.1001	5.57	
M(5)	Al	0	0	0.1248	6.94	
M(6)	Fe, Zn	$\frac{1}{3}$	$\frac{2}{3}$	0.1351	7.51	T_2
M(7)	Fe, Zn	$\frac{2}{3}$	$\frac{1}{3}$	0.1129	6.28	
O(7)	O	0.1470	0.2941	0.1474	8.20	c
O(8)	O	$\frac{2}{3}$	$\frac{1}{3}$	0.1489	8.28	
M(8)	Al	$\frac{1}{3}$	$\frac{1}{6}$	$\frac{1}{6}$	9.27	0

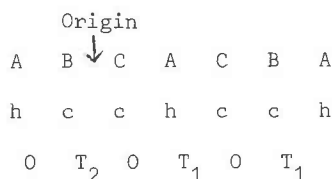


Fig. 6. Anion layer sequence (first two lines) and metal atom layer sequence (third line) for nigerite-6H.

A further consequence of metal atom ordering is an alternation in the magnitude of the oxygen layer separations, corresponding to the T and O metal atom layer alternation. The average oxygen inter-layer separations are about 2.55 and 2.05 Å across T and O metal atom layers respectively. A similar alternation (2.67 and 2.02 Å) was observed in the oxygen layer separations in the (ch...) structure $\text{Co}_2\text{Mn}_3\text{O}_8$ (Riou and Lecerf, 1975).

The site occupancies derived during the structure refinement (Table 3) give a unit-cell composition $\text{Al}_{14.9}\text{Sn}_{2.0}\text{Fe}_{2.8}\text{Zn}_{1.4}\text{O}_{30}(\text{OH})_2$. This is in reasonable agreement with the average composition calculated from the microprobe analysis (Table 2), especially if the minor elements, Si and Mn, are grouped with Al and Fe respectively. The location of the large calcium atom was not ascertained from the structure refinement. It may be distributed over some of the anion sites [calcium occupies an anion site in the close-packed oxide mineral lovingite (Gatehouse *et al.*, 1978)]. Note that the above composition requires some iron as ferric to achieve charge balance. Ferric iron is most likely located with aluminum in the tetrahedral site M(3).

Electrostatic valence sums

Indirect support for partial occupancy of the various sites in nigerite is that the resulting calculated electrostatic valence sums for the oxygens are generally close to theoretical (see Table 7). If we allow for full occupancy of site M(1), oxygen O(1) becomes se-

Table 7. Nigerite-24R: electrostatic valence sums of cations about anions

Anions	Coordination Cations	EVi
O(1)	1 M(1) + M(2) + M(3)	2.02
O(2)	3 M(1)	1.05
O(3)	M(2) + 2 M(4)	1.67
O(4)	M(3) + 3 M(4)	2.15
O(5)	2 M(4) + M(5) + M(6)	2.03
O(6)	3 M(4) + M(6)	2.03
O(7)	M(5) + M(6) + 2 M(8)	2.03
O(8)	M(7) + 3 M(8)	2.05

verely oversaturated, with a ΣVi value of 2.32. Table 7 shows that the O(2) site is occupied by OH, having a ΣVi of 1.05. In the calculation of the unit-cell composition, we thus normalized to 30 O + 2 OH. Finally, the undersaturated O(3) site, $\Sigma\text{Vi} = 1.67$, is reflected in the O(3)-M bonds all being about 0.05 Å shorter than the average values.

Prediction of structures for nigerite-6H and related structures

As discussed above, the correct structural model for nigerite-24R was arrived at using crystallochemical reasoning based on the following principles:

- The structure is based on a close-packed oxygen framework with a mixed (cubic, hexagonal) stacking sequence. The long c_{hex} axis periodicity is due to the ordering sequence of cubic- and hexagonal-stacked layers. This sequence must be consistent with the symmetry and size of the unit cell and the requirement of dominant cubic stacking.
- Between the oxygen layers, ordering of metal atoms gives rise to three possible arrangements, O, T₁, and T₂ (see Fig. 1).
- The sequence of O and T layers is determined by the oxygen-layer stacking sequence. Type O layers must alternate with type T layers. T₁ layers occur between cubic- and hexagonal-stacked oxygen layers. T₂ layers lie between cubic-stacked oxygen layers.
- In the T₁ layers, the unoccupied tetrahedral site is an olivine-like site, *i.e.* sharing the basal edges with three octahedra from the adjacent layer (although partial occupancy of this site may be possible).

Having confirmed these general structural principles for nigerite-24R, it should be possible to apply them to predict the structure of other compounds related to nigerite, but with different c_{hex} axis periodicities. These include other nigerite polytypes, hōgbomites, and taaffeites.

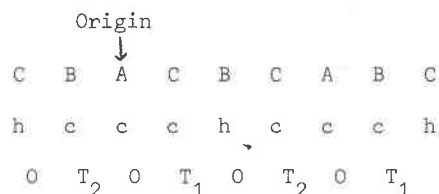


Fig. 7. Anion layer sequence (first two lines) and metal atom layer sequence (third line) for hōgbomite-8H.

An almost trivial example is provided by the six-layer nigerite polytype first described by Bannister *et al.* (1947). This mineral has trigonal symmetry, $\bar{3}m$, with $c = 13.86\text{Å} = 6 \times 2.31\text{Å}$ and with possible space groups $P\bar{3}m1$ or $P\bar{3}1m$. From Table 7.1.5B of Patterson and Kasper (1962), there is only one possible anion layer sequence with dominant cubic stacking. It is designated |(3)|(3)| and has symmetry $P6_3/mmc$ (*i.e.* the trigonal symmetry for nigerite-6H must result from the metal atom arrangement). The oxygen and metal atom layer stacking sequences are given in Figure 6; *i.e.* the oxygen sequence is (cch...) and the metal sequence is $OT_2OT_1OT_1\dots$. Nigerite-6H differs from nigerite-24R in having only two, rather than four, metal layers in the spinel block. If we use the known occupancies in the $\dots OT_1OT_1\dots$ and $\dots OT_2\dots$ blocks obtained for nigerite-24R, we can derive a unit-cell composition for nigerite-6H. Allowing the same fractional occupancies, OH^- at a two-fold site, *etc.* (see Table 3) we have



For comparison, the analysis obtained by Bannister *et al.* (1947) for nigerite-6H is



It appears that in nigerite polytypes the stacking sequence adopted depends on the tin content, *i.e.* the mineral adopts the sequence that allows all the tin atoms to fully occupy (or almost so) the available octahedral sites in T_1 layers. In going from nigerite-24R to nigerite-6H, the ratio of T_1 to T_2 layers increases to accommodate the higher tin content of the latter.

The prediction of the structure for högbomite-8H (*i.e.* högbomite-4H using McKie's nomenclature) is quite straightforward, using the principles listed (a)–(d) above. This mineral has hexagonal symmetry, possible space groups $P6_3mc$, $P\bar{6}2c$, and $P6_3/mmc$, with $c_{\text{hex}} = 18.35\text{Å} = 8 \times 2.29\text{Å}$ (McKie, 1963). From Table 7.1.5B of Patterson and Kasper (1962) the only stacking sequence with dominant cubic stacking is that designated |(4)|(4)|. This has symmetry $P6_3/mmc$, and the origin for the oxygen stacking is located on an oxygen. In order that O and M metal atom layers alternate across the origin oxygen layer, a non-centrosymmetric space group has to be used. The oxygen and metal atom layer sequences are given in Figure 7. Thus, in this structure both the spinel block and the M_5O_8 block are only two metal-atom layers wide. The ideal unit-cell composition (*i.e.* partial occupancy not considered) is $M_{22}O_{32} = M_{5.5}O_8$. Generally, compositions reported for 8H-högbomites contain

higher metal contents and suggest partial occupancy of the second tetrahedral site in the T_1 layers; *e.g.* the composition recently determined for zincian högbomite-8H by Wilson (1977), $(Mg,Fe,Zn,Al,Ti\dots)_{5.762}(O,OH)_8$, requires 50% occupancy of each of the second tetrahedral sites in the T_1 layers. We are currently refining the structure of an 8H-högbomite polytype, and the present *R* factor of ~ 0.08 confirms our correct prediction of the structure using the principles described above.

The taafeite minerals are interesting in that they form 8H and 18R polytypes with similar diffraction patterns to högbomite and nigerite polytypes, but the compositions of both are M_6O_8 , within experimental error (Hudson *et al.*, 1967). In this case it seems the same structural principles apply, but the second tetrahedral site in the T_1 layers is fully occupied, presumably by the very small Be^{2+} ion which compositionally characterizes the taafeite minerals.

Acknowledgments

We thank Mr. L. A. Newnham of Renison Ltd. for supplying the specimens of nigerite, and Mr. P. Kelly, Melbourne University Geology Department, for carrying out the microprobe analyses. We acknowledge the help of Dr. Bruce Poppleton of CSIRO with the computing.

References

- Bannister, F. A., M. A. Hey and H. P. Stadler (1947) Nigerite, a new tin mineral. *Mineral. Mag.*, 28, 129–136.
- Cromer, D. T. and D. Liberman (1970) Relativistic calculation of anomalous scattering factors for X-rays. *J. Chem. Phys.*, 53, 1891–1898.
- and J. B. Mann (1968) X-ray scattering factors computed from numerical Hartree-Fock wave functions. *Acta Crystallogr.*, A24, 321–324.
- Dernier, P. D. and J. P. Remeika (1976) Structural determination of single-crystal K β -alumina and cobalt-doped K β -alumina. *J. Solid. State Chem.*, 17, 245–253.
- Djega-Mariadassou, C., F. Basile, P. Poix and A. Michel (1973) Préparation et propriétés cristallographiques des phases $Fe_{3-x}Sn_xO_4$. *Ann. Chim.*, 8, 15–20.
- Gatehouse, B. M., I. E. Grey, I. H. Campbell and P. Kelly (1978) The crystal structure of loveringite—a new member of the crichtonite group. *Am. Mineral.*, 63, 28–36.
- Hanson, A. W. (1958) The crystal structure of nolanite. *Acta Crystallogr.*, 11, 703–709.
- Hornstra, J. and G. Stubbe (1972) *PW1100 Data Processing Program*. Philips Research Labs, Eindhoven, Holland.
- Hudson, D. R., A. F. Wilson and I. M. Threadgold (1967) A new polytype of taafeite—a rare beryllium mineral from the granulites of central Australia. *Mineral. Mag.*, 36, 305–310.
- Jacobson, R. and J. S. Webb (1947) The occurrence of nigerite, a new tin mineral in quartz-sillimanite-rocks from Nigeria. *Mineral. Mag.*, 28, 118–128.
- Kodama, T. and G. Muto (1976) The crystal structure of $T1$ - β -alumina. *J. Solid State Chem.*, 17, 61–70.

- McCarroll, W. H. (1977) Structural relationships in $A_2Mo_3O_8$ metal atom cluster oxides. *Inorg. Chem.*, *16*, 3351–3353.
- , L. Katz and R. Ward (1957) Ternary oxides of quadrivalent molybdenum. *J. Am. Chem. Soc.* *79*, 5410–5414.
- McKie, D. (1963) The högbomite polytypes. *Mineral. Mag.*, *33*, 563–580.
- Patterson, A. L. and J. S. Kasper (1962) Close packing. In *International Tables for X-ray Crystallography*, Vol. II, chapter 7.1. Kynoch Press, Birmingham.
- Peacor, D. R. (1967) New data on nigerite. *Am. Mineral.*, *52*, 864–866.
- Riou, A. and A. Lecerf (1975) Structure cristalline de $Co_2Mn_3O_8$. *Acta Crystallogr.*, *B31*, 2487–2490.
- Rouse, R. C. and D. R. Peacor (1968) The relationship between senaite, magnetoplumbite and davidite. *Am. Mineral.*, *53*, 869–879.
- Saalfeld, H. (1964) Strukturdaten von Gahnit. *Z. Kristallogr.*, *120*, 476–478.
- Shannon, R. D. and C. T. Prewitt (1969) Effective ionic radii in oxides and fluorides. *Acta Crystallogr.*, *B25*, 925–946.
- Townes, W. D., J. H. Fang and A. J. Perrotta (1967) The crystal structure and refinement of ferrimagnetic barium ferrite, $BaFe_{12}O_{19}$. *Z. Kristallogr.*, *125*, 437–449.
- Wilson, A. F. (1977) A zincian högbomite and some other högbomites from the Strangways Range, Central Australia. *Mineral. Mag.*, *41*, 337–344.

*Manuscript received, October 2, 1978;
accepted for publication, June 26, 1979.*